

# Measurements of the Vapor–Liquid Equilibrium for the CO<sub>2</sub> + R290 Mixture

Katsuyuki Tanaka,<sup>\*,†</sup> Yukihiro Higashi,<sup>†</sup> Ryo Akasaka,<sup>‡</sup> Yohei Kayukawa,<sup>§</sup> and Kenich Fujii<sup>§</sup>

Department of Mechanical Systems and Design Engineering, Iwaki Meisei University, Iwaki, Fukushima 970-8551, Japan, Faculty of Humanities, Kyushu Lutheran College, Kumamoto 860-8520, Japan, and Fluid Property Section, Material Properties and Metrological Statistics Division, National Metrology Institute of Japan, National Institute of Advanced Industrial Science and Technology, Tsukuba 305-8563, Japan

Vapor–liquid equilibrium (VLE) of the CO<sub>2</sub> + R290 mixture has been measured by the recirculation method. Thirty-three data sets of VLE measurements were obtained in the temperature range between (260 and 290) K and in the pressure range between (408 and 4710) kPa. The experimental uncertainties of the temperature, pressure, and composition measurements are estimated to be within 3 mK, 3 kPa, and 0.11 %, respectively. The present data were compared with the calculation by the REFPROP and correlated well by two cubic equations of state, i.e., the Peng–Robinson equation and the Soave–Redlich–Kwong equation.

## Introduction

Due to global environmental issues such as ozone depletion and global warming, production of fluorocarbon refrigerants that are typical working fluids of refrigerators and heat pump systems will be regulated. Suitable alternative refrigerants including hydrocarbons such as R290 (propane: C<sub>3</sub>H<sub>8</sub>) and R600a (isobutane: *i*-C<sub>4</sub>H<sub>10</sub>) have focused attention as natural refrigerants. A home-type refrigerator with R600a has already been in the Japanese marketplace. However, usage of a large amount of hydrocarbons in air-conditioning remains a problem because of its flammability. Carbon dioxide (CO<sub>2</sub>) is also a natural refrigerant and is used as a working fluid in heating of heat pump systems. The application of CO<sub>2</sub> as a refrigerant remains an issue due to its operation under high pressure.

To improve the above issues, natural refrigerant mixtures such as CO<sub>2</sub> + hydrocarbons were an interest in our research target. In recent years, thermophysical properties for mixtures composed of R290, R600a, and R32 (difluoromethane: CH<sub>2</sub>F<sub>2</sub>) have been measured in our laboratory. Vapor–liquid equilibrium measurements were conducted for R290 + R600a,<sup>1</sup> R290 + R32,<sup>2</sup> and R600a + R32.<sup>3</sup> Critical parameters and saturated density measurements were conducted for R290 + R600a,<sup>4</sup> R290 + R32,<sup>5</sup> and R600a + R32.<sup>6</sup> Surface tension measurement was conducted for R290 + R600a.<sup>7</sup> As the first stage in our target of mixtures containing R290, R600a, and CO<sub>2</sub>, VLE measurements of the CO<sub>2</sub> + R290 mixture have been studied.

In the present study, the vapor–liquid equilibrium measurements for CO<sub>2</sub> + R290 were carried out from (260 to 290) K and compared with available literature data and REFPROP.<sup>8</sup> By using the present data, the interaction parameters  $k_{ij}$  for two cubic equations of state, i.e., Peng–Robinson equation of state (PR EOS)<sup>9</sup> and Soave–Redlich–Kwong equation of state (SRK EOS),<sup>10</sup> were determined. The present data and literature data were also compared with the above two equations of state.

\* To whom correspondence should be addressed. E-mail: ktanaka@iwakimu.ac.jp. Tel.: +81-246-29-7026. Fax: +81-246-29-0577.

<sup>†</sup> Iwaki Meisei University.

<sup>‡</sup> Kyushu Lutheran College.

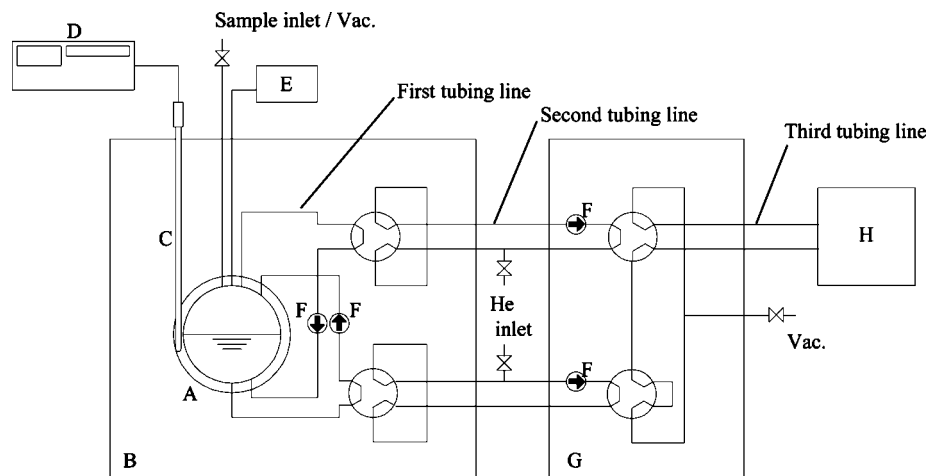
<sup>§</sup> National Institute of Advanced Industrial Science and Technology.

Table 1. Experimental Uncertainties

property	source	uncertainty
temperature	thermometer	1 mK
	fluctuation	1 mK
	expanded uncertainty ( $k = 2$ )	3 mK
pressure	repeatability	0.5 kPa
	calibration	1 kPa
	expanded uncertainty ( $k = 2$ )	3 kPa
composition	calibration	0.02 mol %
	repeatability	0.05 mol %
	expanded uncertainty ( $k = 2$ )	0.11 mol %

## Experimental Apparatus

The measurements were carried out using the recirculation method that had been previously employed to measure vapor–liquid equilibrium for the binary mixtures composed of R290, R600a, and R32.<sup>1–3</sup> Since the apparatus and experimental procedures have been described in detail in our previous publication,<sup>1</sup> an overview is presented here. A schematic diagram of the apparatus is shown in Figure 1. A sample of the first component is loaded into the equilibrium cell, which has optical windows to confirm the meniscus of the sample. A sample of the second component can be loaded into the equilibrium cell. Saturated vapor is circulated from the top of the equilibrium cell to the bottom of the cell through a sampling tubing line equipped with a magnetic circulation pump. Saturated liquid is circulated from the bottom of the equilibrium cell to the top of the cell through another sampling tubing line in the same way. The equilibrium cell and sampling tubing lines are immersed in the thermostatted liquid bath, whose heat-transfer medium is ethylene glycol. The temperature of the thermostatted liquid bath was measured by using the precise thermometer bridge (ASL, F17A) and 100 Ω standard platinum resistance thermometer (Netsushin, NSR-300) calibrated against ITS-90. The uncertainty of temperature measurement is estimated to be within 3 mK. The sample pressure was measured using a quartz pressure transducer (Paroscientific, 2900AT), which is attached at the top of the equilibrium cell. The uncertainty of pressure measurement is estimated to be within 3 kPa. After the measurements of sample temperature and pressure, the saturated vapor and saturated liquid were extracted from the sampling



**Figure 1.** Schematic diagram of the experimental apparatus: A, equilibrium cell; B, thermostatted liquid bath; C, platinum resistance thermometer; D, precise thermometer bridge; E, pressure transducer; F, circulation pump; G, thermostatted air bath; H, gas chromatograph.

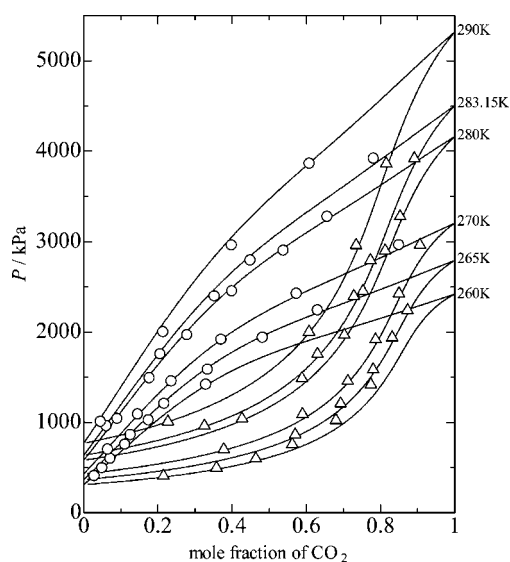


**Figure 2.** Vapor-liquid equilibrium for the CO<sub>2</sub> + R290 mixture on a pressure-composition diagram: O, bubble-point data; Δ, dew-point data. —, isotherm of the bubble-point and dew-point pressure calculated by REFPROP.<sup>8</sup>

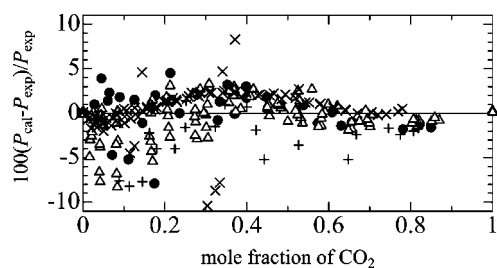


**Figure 3.** Bubble-point pressure deviation between the experimental data and the REFPROP calculations against composition: ●, present study; Δ, Kim;<sup>13</sup> ×, Niesen;<sup>14</sup> +, Hamam.<sup>15</sup>

tubing line using the hexagon valve to the secondary tubing lines. The sample is pressurized by introducing high-purity (99.999 %) helium gas in the secondary tubing lines. Secondary tubing lines lead to the thermostatted air bath next to the liquid bath. Saturated vapor and saturated liquid in the secondary tubing lines are sequentially extracted using the hexagon valve to the third tubing line, which is connected to the gas chromatograph (Agilent Technologies, 6890N) with a Porapak-Q column (2 m long; ID 3 mm; mesh range 50/50) for the

**Table 2.** Experimental Results of Vapor-Liquid Equilibrium for the CO<sub>2</sub> + R290 Mixture

<i>T</i>	<i>P</i>	<i>x</i>	<i>y</i>
K	kPa	mol·mol <sup>-1</sup>	mol·mol <sup>-1</sup>
260.000	409	0.028	0.215
260.000	496	0.049	0.378
260.000	600	0.071	0.464
260.000	757	0.111	0.562
260.000	1025	0.175	0.680
260.000	1420	0.329	0.774
265.000	863	0.126	0.570
265.000	1209	0.217	0.692
265.000	1585	0.334	0.780
265.000	1940	0.482	0.831
265.000	2241	0.631	0.873
270.000	702	0.065	0.378
270.000	1091	0.146	0.590
270.000	1457	0.236	0.712
270.000	1918	0.370	0.787
270.000	2426	0.574	0.850
270.000	2964	0.850	0.906
280.000	1042	0.090	0.427
280.000	1491	0.177	0.588
280.000	1967	0.278	0.703
280.000	2452	0.399	0.753
280.000	2902	0.538	0.813
280.000	3278	0.657	0.853
283.150	961	0.061	0.325
283.150	1757	0.206	0.630
283.150	2398	0.352	0.728
283.150	2794	0.449	0.773
283.150	3921	0.781	0.891
290.000	1009	0.045	0.227
290.000	2002	0.214	0.607
290.000	2961	0.399	0.734
290.000	3865	0.608	0.815
290.000	4710	0.823	0.881

determination of compositions in the saturated vapor and liquid. The uncertainty of the composition measurement is estimated to be within 0.11 mol %. The sources of the uncertainty in the VLE measurement are summarized in Table 1.

CO<sub>2</sub> was manufactured by Showa Tansan Co., Ltd. Its sample purity is stated more than 99.999 vol %. R290 was manufactured by Takachiho Co., Ltd. Its sample purity is more than 99.99 mol %. No further purification was done on the samples before use.

## Results and Discussion

**Comparison with Literature Data.** The vapor-liquid equilibrium for the CO<sub>2</sub> + R290 mixture was measured in the

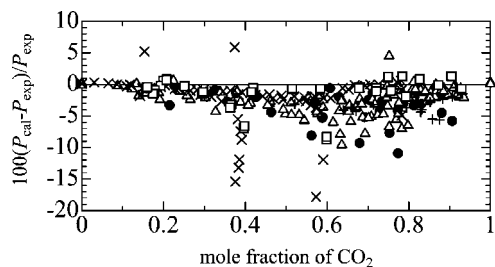


**Figure 4.** Dew-point pressure deviation between the experimental data and the REFPROP calculations against composition: ●, present study; △, Kim;<sup>13</sup> ×, Niesen;<sup>14</sup> +, Hamam;<sup>15</sup> □, Reamer.<sup>16</sup>

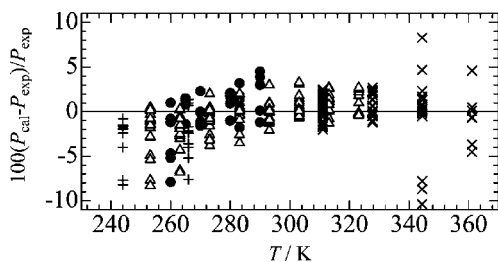


**Figure 5.** Bubble-point pressure deviation between the experimental data and the REFPROP calculations against temperature: ●, present study; △, Kim;<sup>13</sup> ×, Niesen;<sup>14</sup> +, Hamam.<sup>15</sup>

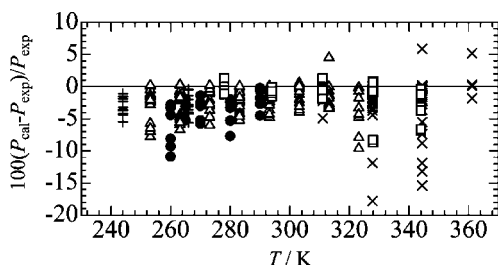


**Figure 6.** Dew-point pressure deviation between the experimental data and the REFPROP calculations against temperature: ●, present study; △, Kim;<sup>13</sup> ×, Niesen;<sup>14</sup> +, Hamam;<sup>15</sup> □, Reamer.<sup>16</sup>

temperature range from (260 to 290) K and in the pressure range between (408 and 4710) kPa. The experimental results are given in Table 2. The distribution of the present VLE data is shown in Figure 2 on the  $P-x$  diagram, which indicates that this mixture is nonazeotropic. The deviations of the bubble point and dew point pressure of the present data from the calculations by REFPROP<sup>8</sup> against composition are shown in Figures 3 and 4, and those against temperature are shown in Figures 5 and 6. REFPROP was adopted for the Kunz and Wagner model<sup>11</sup> for this system. The literature data are also included in Figures 3 to 6, but the data by Acosta et al.<sup>12</sup> were removed because of their large deviations. The experimental range of the present data and the literature data is shown in Table 3.  $U_T$ ,  $U_P$ , and  $U_{x,y}$  in Table 3 are the uncertainties of temperature, pressure, and composition, respectively. The statistical characteristics (AAD, BIAS, and RSD) of the percent deviations of the literature data and present data from the REFPROP calculations are summarized in Table 4. The AAD, BIAS, and RSD are defined as the following equations.

$$\text{AAD} = \frac{1}{n} \sum_{i=1}^n \left| \frac{P_{\text{cal}} - P_{\text{exp}}}{P_{\text{exp}}} \right| \cdot 100 \quad (1)$$

$$\text{BIAS} = \frac{1}{n} \sum_{i=1}^n \left( \frac{P_{\text{cal}} - P_{\text{exp}}}{P_{\text{exp}}} \right) \cdot 100 \quad (2)$$

$$\text{RSD} = \sqrt{\frac{1}{n-1} \sum_{i=1}^n \left( \frac{P_{\text{cal}} - P_{\text{exp}}}{P_{\text{exp}}} \cdot 100 - \text{BIAS} \right)^2} \quad (3)$$

Although the bubble-point pressure of the present data is in a good agreement with REFPROP calculations, the dew-point pressure of the present data is always bigger than the REFPROP calculations. The BIAS for the dew-point pressure is  $-3.63\%$ , whereas that for bubble-point pressure is  $0.21\%$ . As shown in Figure 4, the difference between the dew-point pressure of the present data and the REFPROP calculations becomes slightly larger in the region of  $\text{CO}_2$ -rich composition. The data by Acosta et al.,<sup>12</sup> which were obtained in the temperature range from (210.9 to 349.8) K, show the largest statistical characteristic in all data. The reason for this is a relatively large experimental

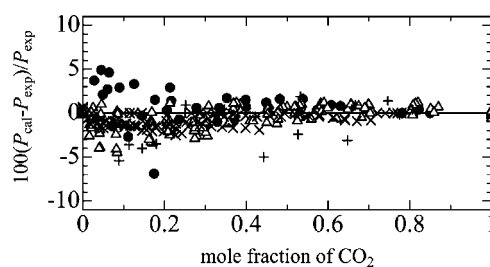


**Figure 7.** Bubble-point pressure deviation between the experimental data and PR EOS against composition: ●, present study; △, Kim;<sup>13</sup> ×, Niesen;<sup>14</sup> +, Hamam.<sup>15</sup>

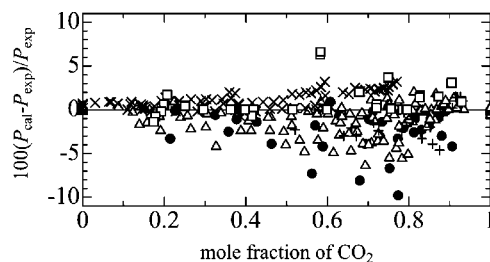


**Figure 8.** Dew-point pressure deviation between the experimental data and PR EOS against composition: ●, present study; △, Kim;<sup>13</sup> ×, Niesen;<sup>14</sup> +, Hamam;<sup>15</sup> □, Reamer.<sup>16</sup>

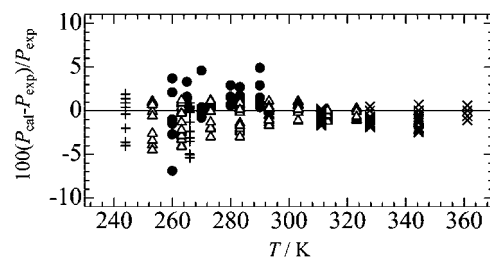


**Figure 9.** Bubble-point pressure deviation between the experimental data and PR EOS against temperature: ●, present study; △, Kim;<sup>13</sup> ×, Niesen;<sup>14</sup> +, Hamam.<sup>15</sup>

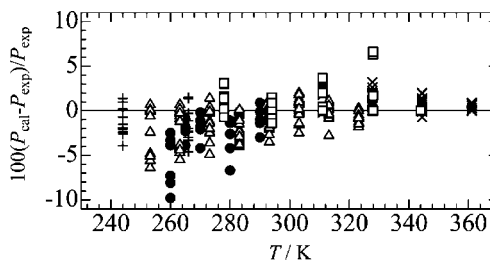


**Figure 10.** Dew-point pressure deviation between the experimental data and PR EOS against temperature: ●, present study; △, Kim;<sup>13</sup> ×, Niesen;<sup>14</sup> +, Hamam;<sup>15</sup> □, Reamer.<sup>16</sup>

Table 3. Experimental Range of the Present Data and the Literature Data

first author	N	Experimental Range					
		T K	U <sub>T</sub> K	P kPa	U kPa	x, y mol·mol <sup>-1</sup>	U <sub>x, y</sub> %
Bubble-Point Pressure							
present work	33	260 to 290	0.003	409 to 4710	3	0.02 to 0.85	0.11
Acosta <sup>12</sup>	144	210 to 346	0.05	289 to 5859	15	0.07 to 0.45	0.1
Hamam <sup>15</sup>	21	244 to 266	0.11	503 to 2613	(0.27 to 0.53) %	0.08 to 0.82	0.3
Kim <sup>13</sup>	124	253 to 324	0.02	244 to 7207	1	0.00 to 1.00	0.3
Niesen <sup>14</sup>	94	311 to 362	0.1	1302 to 6702	0.05 %	0.00 to 0.78	0.2
Dew-Point Pressure							
present work	33	260 to 290	0.003	409 to 4710	3	0.21 to 0.91	0.11
Acosta <sup>12</sup>	145	210 to 350	0.05	59 to 3483	15	0.07 to 0.45	0.1
Hamam <sup>15</sup>	21	244 to 266	0.11	503 to 2613	(0.27 to 0.53) %	0.52 to 0.94	0.3
Kim <sup>13</sup>	124	253 to 324	0.02	244 to 7207	1	0.00 to 1.00	0.3
Niesen <sup>14</sup>	94	311 to 362	0.1	1302 to 6702	0.05 %	0.00 to 0.80	0.2
Reamer <sup>16</sup>	44	278 to 344	0.011	685 to 6716	0.1 % or 2.1 kPa	0.15 to 0.93	0.3

Table 4. Relative Pressure Deviation of the Bubble-Point and Dew-Point Pressure for the CO<sub>2</sub> + R290 Mixture from the REFPROP<sup>8</sup>

first author	REFPROP		
	AAD %	BIAS %	RSD %
Bubble-Point Pressure			
present work	1.97	0.21	2.59
Acosta <sup>12</sup>	18.88	-17.19	22.35
Hamam <sup>15</sup>	3.18	-2.88	2.72
Kim <sup>13</sup>	1.43	-0.49	2.08
Niesen <sup>14</sup>	1.57	0.41	2.43
Dew-Point Pressure			
present work	3.63	-3.63	2.49
Acosta <sup>12</sup>	11.61	3.54	13.14
Hamam <sup>15</sup>	3.00	-3.00	1.50
Kim <sup>13</sup>	1.73	-1.69	1.79
Niesen <sup>14</sup>	2.04	-1.75	3.52
Reamer <sup>16</sup>	1.53	-1.07	2.35

Table 5. Relative Pressure Deviation of the Bubble-Point and Dew-Point Pressure for the CO<sub>2</sub> + R290 Mixture from Two Cubic Equations of State (PR EOS and SRK EOS)

first author	PR EOS			SRK EOS		
	$k_{ij} = 0.1276$			$k_{ij} = 0.1333$		
	AAD %	BIAS %	RSD %	AAD %	BIAS %	RSD %
Bubble-Point Pressure						
present work	1.73	0.88	2.17	1.80	1.00	2.20
Acosta <sup>12</sup>	16.37	-16.27	19.58	16.47	-16.39	19.64
Hamam <sup>15</sup>	1.81	-1.17	2.19	1.92	-0.85	2.34
Kim <sup>13</sup>	1.03	-0.50	1.31	1.24	-0.39	1.48
Niesen <sup>14</sup>	0.84	-0.79	0.75	1.07	-0.94	1.01
Dew-Point Pressure						
present work	2.74	-2.68	2.42	2.90	-2.78	2.53
Acosta <sup>12</sup>	11.79	4.24	13.08	12.56	4.30	13.44
Hamam <sup>15</sup>	2.03	-1.51	1.79	2.39	-1.77	2.02
Kim <sup>13</sup>	1.38	-1.06	1.72	1.74	-1.35	1.95
Niesen <sup>14</sup>	1.00	0.96	0.97	0.61	0.19	0.83
Reamer <sup>16</sup>	1.07	0.93	2.61	0.77	0.68	0.93

uncertainty in pressure measurements due to small absolute pressures in the low-temperature region. The data by Kim and Kim<sup>13</sup> were obtained in the wide temperature range from (253.15 to 323.15) K. Their data show a behavior similar to the present data over the whole range of mole fraction of CO<sub>2</sub> as shown in Figures 3 and 4. The data by Niesen and Rainwater<sup>14</sup> were obtained in the temperature range from (310 to 361) K and the pressure range from the vapor pressure up to the critical pressure. Although both AAD and BIAS of the data are small, the deviations from the REFPROP calculation become larger near the critical point as shown in Figures 5 and 6. The data by

Hamam and Lu<sup>15</sup> were obtained in the temperature range from (244 to 266) K. The data for bubble-point and dew-point pressure show large negative BIAS, and their behavior is dissimilar to other data. The data by Reamer and Sage<sup>16</sup> were obtained only for the dew-point pressure in the temperature range from (278 to 344) K. Their data are in a good agreement with REFPROP calculations.

As shown in the comparison of the present data with the REFPROP, its deviation of the dew-point pressure is negative, especially in the region of CO<sub>2</sub>-rich composition (Figure 4), and decreasing at lower temperature (Figure 6). The data by Kim and Kim show behavior similar to the present data and are useful to correlate with cubic equations of state.

**Correlation by Cubic Equations of State.** The present VLE data were correlated with two cubic equations of state, i.e., PR EOS<sup>9</sup> and SRK EOS,<sup>10</sup> with the mixing rule expressed as follows.

$$a = \sum_i \sum_j x_i x_j a_{ij} \quad (4)$$

$$a_{ii} = a_i, \quad a_{jj} = a_j, \quad a_{ij} = a_{ji} = (1 - k_{ij}) \sqrt{a_i a_j} \quad (5)$$

$$b = \sum_i x_i b_i \quad (6)$$

$$c = \sum_i x_i c_i \quad (7)$$

where  $k_{ij}$  is the binary interaction parameter. The binary interaction parameters  $k_{ij}$  were determined for two equations of state. A total of 143 data sets of ( $T, P, x, y$ ) based on the present data and the data by Kim and Kim<sup>13</sup> were used. The ( $T, x$ ) data sets were used as the input data, and the  $k_{ij}$  were determined to minimize the bubble-point pressure deviation by the least-squares method. The  $k_{ij}$  values thus obtained are summarized in Table 5 as well as the statistical characteristics. The deviations of the bubble-point and dew-point pressure of the present data from the calculations by PR EOS against composition are shown in Figures 7 and 8, and those against temperature are shown in Figures 9 and 10. The optimum values of  $k_{ij}$  for PR EOS and SRK EOS are almost the same with a value of 0.13. The two EOS with the optimum  $k_{ij}$  give almost the same statistical characteristics, which are improved from those of the REFPROP calculations. The improvements in AAD are 1.0 % for the bubble-point pressure and 0.5 % for the dew-point pressure. Especially, as shown in figures related to dew-point pressure deviation, the accuracy for the dew-point pressure was improved.

## Conclusion

The VLE measurements for the CO<sub>2</sub> + R290 mixture were performed in the temperature range from (260 to 290) K, and 33 data sets of (*T*, *P*, *x*, *y*) were obtained. By using two cubic equations of state (PR EOS and SRK EOS), the VLE data were correlated. The optimum binary interaction parameter *k<sub>ij</sub>* for each equation of state was determined. It is found that the VLE of CO<sub>2</sub> + R290 mixtures can be successfully represented by the cubic equations of state with the optimum *k<sub>ij</sub>*.

## Literature Cited

- (1) Kayukawa, Y.; Fujii, K.; Higashi, Y. Vapor-Liquid Equilibrium (VLE) Properties for the Binary Systems Propane (1) + n-Butane (2) and Propane (1) + Isobutane (3). *J. Chem. Eng. Data* **2005**, *50*, 579–582.
- (2) Higashi, Y. Vapor-Liquid Equilibria For The Binary Difluoromethane (R-32) + Propane (R-290) Mixture. *Int. J. Thermophys.* **1999**, *20*, 507–518.
- (3) Akasaka, R.; Higashi, Y.; Tanaka, K.; Kayukawa, Y.; Fujii, K. Vapor-liquid equilibrium measurements and correlations for the binary mixture of difluoromethane + isobutane and the ternary mixture of propane + isobutane + difluoromethane. *Fluid Phase Equilib.* **2007**, *261*, 286–291.
- (4) Higashi, Y. Measurements of saturated densities and critical parameters for the propane+isobutane system. *Proc. IIR-Gustav Lorentzen Conf.* **2004**, 128–135.
- (5) Higashi, Y. Experimental Determination of the Critical Locus for the Difluoromethane (R32) and Propane (R290) System. *Fluid Phase Equilib.* **2004**, *219*, 99–103.
- (6) Higashi, Y. Composition dependence of the critical parameters for the binary mixtures of R32 + R290, R32 + R600a, and R290 + R600a system. *Proc. IIR Int. Conf.* **2005**, 153–159.
- (7) Tanaka, K.; Higashi, Y. Measurements of the surface tension for R290, R600a and R290/R600a mixture. *Int. J. Refrig* **2007**, *20*, 1368–1373.
- (8) Lemmon, E. W.; Huber, M. L.; McLinden, M. O. *NIST Standard Reference Data 23 REFPROP ver. 8.0*; 2007.
- (9) Peng, D. Y.; Robinson, D. B. A new two-constant equation of state. *Ind. Eng. Chem. Fundam.* **1976**, *15*, 59–64.
- (10) Soave, G. Equilibrium constants from modified Redlich-Kwong equation of state. *Chem. Eng. Sci.* **1972**, *27*, 1197–1203.
- (11) Kunz, O.; Klimeck, R.; Wagner, W.; Jaeschke, M. *GERG Technical Monograph 15*; VDI Verlag: Düsseldorf, 2007.
- (12) Acosta, J. C.; Hevia, E.; Leipziger, S. Dew and bubble point measurements for carbon dioxide-propane mixtures. *J. Chem. Eng. Data* **1984**, *29*, 304–309.
- (13) Kim, J. H.; Kim, M. S. Vapor-liquid equilibria for the carbon dioxide + propane system over a temperature range from 253.15 to 323.15 K. *Fluid Phase Equilib.* **2005**, *238*, 13–19.
- (14) Niesen, V. G.; Rainwater, J. C. Critical locus, (vapor + liquid) equilibria, and coexisting densities of (carbon dioxide + propane) at temperatures from 311 to 361 K. *J. Chem. Thermodyn.* **1990**, *22*, 777–795.
- (15) Hamam, S. E. M.; Lu, B. C.-Y. Isothermal vapor-liquid equilibria in binary system propane-carbon dioxide. *J. Chem. Eng. Data* **1976**, *21*, 200–204.
- (16) Reamer, H. H.; Sage, B. H. Volumetric and phase behavior of the propane-carbon dioxide system. *Ind. Eng. Chem.* **1951**, *43*, 2515–2520.

Received for review December 3, 2008. Accepted January 20, 2009.

JE800938S